Composites: Part A 106 (2018) 82–90

Contents lists available at ScienceDirect

Composites: Part A

journal homepage: www.elsevier.com/locate/compositesa

Impact resistance of shear thickening fluid/Kevlar composite treated with shear-stiffening gel

Qianyun He, Saisai Cao, Yunpeng Wang, Shouhu Xuan *, Pengfei Wang, Xinglong Gong *

CAS Key Laboratory of Mechanical Behavior and Design of Materials, Department of Modern Mechanics, University of Science and Technology of China (USTC), Hefei 230027, PR China

ARTICLE INFO

Article history:
Received 28 June 2017
Received in revised form 12 December 2017
Accepted 19 December 2017
Available online 20 December 2017

Keywords:
A. Nanocomposites
B. Impact behavior
D. Mechanical testing
Shear thickening

ABSTRACT

In this work, shear-stiffening gel (STG) was introduced into shear thickening fluid (STF)-impregnated-Kevlar® woven fabric (Kevlar/STF) to improve the impact resistance. The STF filled within the yarns of Kevlar and the STG covered the Kevlar/STF to form Kevlar/STF/STG composite. The STG in the Kevlar/STF/STG not only protected STF but also improved the impact resistance of the fabric because of its excellent shear-stiffening characteristics. A series of experiments including the yarn pull-out test, the split Hopkinson pressure bar impact test, rod penetration test, and knife cutting test were carried out to verify the enhancement effect. The improvement mechanism of the impact resistance for the Kevlar/STF/STG was studied. Under the similar anti-impact performance, the Kevlar/STF/STG possessed lower weight than the Kevlar and its strong impact resistance originated from the synergetic effect among the STF, STG and Kevlar. Therefore, the Kevlar/STF/STG exhibited broad potential in the soft body armor.

1. Introduction

Body armor, which is designed to weaken slashing or penetrating attacks, mainly consist of hard-plate reinforced body armor and soft non-plated body armor. The hard one can protect high-risk areas from the impact of high-speed bullet. Since the main part is a ceramic or steel plate, the cumbersome nature restricts the movement of the wearer. The soft one mainly protects the arms and legs against the low-speed impact. Usually, it is prepared with multi-layer woven fabrics [1]. These fabrics are usually made of high performance fibers (such as Kevlar, Twaron, Spectra, Dyneema) with high strength, large modulus and low density [1,2]. Because the stacked multilayer fabrics are still heavy, how to reduce the weight of soft body armor under the same protective effect become a challenge.

Wagner et al. firstly introduced the shear thickening fluid (STF) into aramid Kevlar® woven fabric to develop the STF/Kevlar soft armor and they found that the STF significantly improved the ballistic performance of Kevlar [2]. The STF is a kind of densely packed suspensions whose viscosity increases rapidly with the increasing of shear rate or shear stress. When subjected to high-speed impact, the STF transits from liquid to solid-like state and returns to the initial liquid state when the external force disappears [3,4]. Due to the typical shear thickening behavior, STF can be used in damping devices and soft armor [5,6]. Inspired by the Wagner's idea, various in-depth investigations on the mechanical properties of the Kevlar/STF were carried out. Both experiment tests and numerical simulations indicate that the impact resistance of the Kevlar/STF is much stronger than pure Kevlar fabric [7–14]. It is found that the impact resistance of Kevlar/STF is affected by various factors, such as the dispersed particle type, hardness, concentration in STF, dispersing medium type, solvent ratio on STF, additives (such as, silicon carbide, carbon nanotubes), padding pressure, the weave of fabric construction and the change of shot location [15–21]. However, although the Kevlar/STF exhibites high protecting performance, some shortcomings are still exist. Firstly, the STFs are prepared by dispersing the particles in a hygroscopic liquid, such as ethylene glycol, PEG200. Once the STF is long-timely exposed to the air, the shear thickening performance will be reduced because it absorbs water in the moisture. Secondly, part of the fluidic STF will inevitably lost in the Kevlar/STF without any protection. Therefore, more work should be done to improve the stability of the Kevlar/STF.

The shear-stiffening gel (STG) is a typical visco-elastic material [22] whose mechanical properties, such as storage modulus, elastic modulus and yield stress, are critically enhanced under applying the external forces (quasi-static compression, shear loading, dynamic shear loading, and high strain rate compression) [22–24]. As the strain rate increases, the STG changes from the viscous liquid to the rubbery state, and then becomes a glassy state. During the transition, the impact energy is absorbed to against

* Corresponding authors.
E-mail addresses: xuansh@ustc.edu.cn (S. Xuan), gongxl@ustc.edu.cn (X. Gong).

https://doi.org/10.1016/j.compositesa.2017.12.019
1359-835X/

the deformation, thus the STG exhibits good impact protection performance [25]. By introducing different additives, such as borax, silicates, magnetic carbonyl iron particles, multi-walled carbon nanotubes, multifunctional STG with magnetic-mechanical or electric-mechanical coupling behaviors can be successfully obtained [26,27]. Very recently, our group developed a novel STG/MWCNT/Kevlar-based wearable electronic sensing textile by doping the STG and MWCNT into the Kevlar fabric. The safeguarding performance of the Kevlar/MWCNT can be significantly enhanced by STG due to its excellent shear stiffening character [28]. In consideration of the gel-like state, the STG will be favorable to protect the STF from the moisture after doping them into the Kevlar/STF. Therefore, high impact protecting performance will be expected by impregnating the STG into the Kevlar/STF composite.

In this work, the novel STG doped Kevlar/STF was developed to form Kevlar/STF/STG composite and its anti-impact performance was investigated. In comparison to the Kevlar/STF, the Kevlar/STF/STG composite exhibited better mechanical properties. A series of experiments, including the yarn pull-out test, the modified split Hopkinson pressure bar (SHPB) impact test, rod penetration test, and knife cutting test, were carried out to verify the enhancement effect. The enhancing mechanism of the impact resistance was systematically analyzed. At last, different doping methods were compared and the relative improvement nature was discussed.

2. Experimental

2.1. Materials

The materials included tetraethyl orthosilicate (TEOS), aqueous ammonia solution ($NH_3{\cdot}H_2O$), ethanol, polyethylene glycol (PEG200), ethylene glycol (EG), boric acid, dimethyl silicone oil, benzoyl peroxide (BPO), acetone. The reagents mentioned above were all purchased from Sinopharm Chemical Reagent Co., Ltd., and used without further purification. The high-performance fibers Kevlar®129 were woven into plain weave fabrics (1000 denier, 22.5 yarns per inch, Beijing Junantai Protection Technology Co., Ltd., China) with an areal density of 200 g/m^2. Two kinds of particles were used to prepare STF. (a) The silica nanospheres with an average diameter of 230 nm (SiO_2) (Fig. 1b) were synthesized following the sol-gel method. (b) silica particles with an average diameter of 2.6 μm ($mSiO_2$) (Fig. 8a inset) were obtained from industrial grinding.

2.2. Preparation of fabric composites

Synthesis of SiO_2 nanospheres: ethanol (500 mL), deionized water (50 mL) and $NH_3{\cdot}H_2O$ (50 mL) were mixed at 30 °C, and TEOS (50 mL) was quickly added after 30 min. The reaction was maintained with mechanical stirring for 12 h. The SiO_2 nanoparticles were collected by centrifugation, washing, dried in a vacuum oven and milled to powder.

Preparation of STF and mSTF: the most commonly used STF in this work was prepared by dispersing the nanospheres SiO_2 in PEG200 with a fraction of 60 vol%. Besides, the micron-sized $mSiO_2$ were dispersed in EG to prepare mSTF with a fraction of 56 vol%.

Preparation of STG: boric acid was heated at 160 °C for 2 h to form pyroboric acid. Then, the pyroboric acid, dimethyl silicone oil, and ethanol were mixed (at a ratio of 2 g:15 g:1 mL) and reacted at 240 °C. 9 h later, the reaction system was cooled down to get the polymer precursor. The STG was obtained by mixing the precursor with BPO at a ratio of 25:1 and then be vulcanized at 95 °C for 2 h.

Preparation of Kevlar/STF composite: the STF was diluted with ethanol (1:4). The fabrics which could be cut into different sizes were immersed in the diluted solution for 3 min, and placed in an oven at 60 °C for 1 h to evaporate the ethanol.

Preparation of Kevlar/STF/STG composite: Kevlar/STF/STG was fabricated by a "dip and dry" method. The above polymer matrix and BPO were dissolved in 200 mL of acetone at a ratio of 25:1. Then, the Kevlar/STF was dipped in the homogeneous mixture for 5 s, dried in an oven at 40 °C for 30 min, and vulcanized at 95 °C for 2 h.

Preparation of Kevlar/STF/STG (hlm) composite: a more straightforward approach was used. The STG was directly placed on the Kevlar/STF by "hand layup method", and the composite was abbreviated as Kevlar/STF/STG (hlm).

To simplify the description, Kevlar/STF(x) means that the mass ratio of Kevlar to STF is 1:x, and Kevlar/STF(y)/STG(z) represents the ratio of three components is 1:y:z.

2.3. Material characterization

First, the macroscopic and microscopic morphological characterization of the material was carried out. Fig. 1a showed the photographs of STF, STG, and Kevlar/STF/STG composite. The fluidic STF prepared by 230 nm SiO_2 was a white suspension. The STG was solid and its shape changed under the gravity thus it showed a cold flow behavior. Because the weight ratios of the STF and STG in the Kevlar/STF/STG were very small, the visual appearance of Kevlar/STF/STG was similar to the neat Kevlar. The morphology of the 230 nm SiO_2 in STF and Kevlar/STF was observed using a scanning electron microscope (SEM, JEOL JSM-6700F). After the STF was immersed into Kevlar, the dispersant would evaporate in high vacuum. It was found that a large number of particles were distributed on the surface of the filaments, and the particle size was much smaller than the diameter of filaments (Kevlar/STF in Fig. 1c and d). Fig. 1e and f showed the SEM image of Kevlar/STF/STG, which indicated that the STG covered the surface of the SiO_2-attached-filaments and fulfilled the gap between the filaments, thus increased the interconnection between the filaments. To clearly understand the interaction among the three components, a scheme for the cross-sectional structure of the Kevlar/STF/STG was shown in Fig. 2. The SiO_2 particles in the STF were mainly distributed on the surface of the filaments, while STG covered the surface of the Kevlar/STF filaments. Clearly, the STG isolated the STF from the air.

The rheological properties of the STF and STG were tested using a controlled-stress rheometer (Anton Paar MCR 301). A cone-plate geometry with a cone angle of 2° and a diameter of 25 mm was used for testing STF, while a parallel-plate geometry with a diameter of 20 mm was selected for STG. The viscosity *vs.* shear rate curve for the 60 vol% STF under steady shear (Fig. 3a) indicated a significant shear thickening behavior. With the increment of shear rate from 11.8 to 55.1 1/s, the viscosity increased from 15.1 to 1310 Pa·s. Fig. 3b depicted the storage modulus and loss modulus of STG under dynamic oscillatory shear ($\gamma = 1\%$). The shear frequency varied from 10^{-1} to 10^2 Hz, while the storage modulus changed from 324 Pa to 1.02 MPa. Obviously, the STG showed a typical shear stiffening character and it changed from viscous state to elastic state under shear.

2.4. Yarn pull-out test

Yarn pull-out test was used to study the effect of STF and STG additives on the friction between yarns. The composite fabrics were cut into pieces with a size of 80 × 50 mm^2. Table 1 listed the composition and mass ratio of different composite fabrics

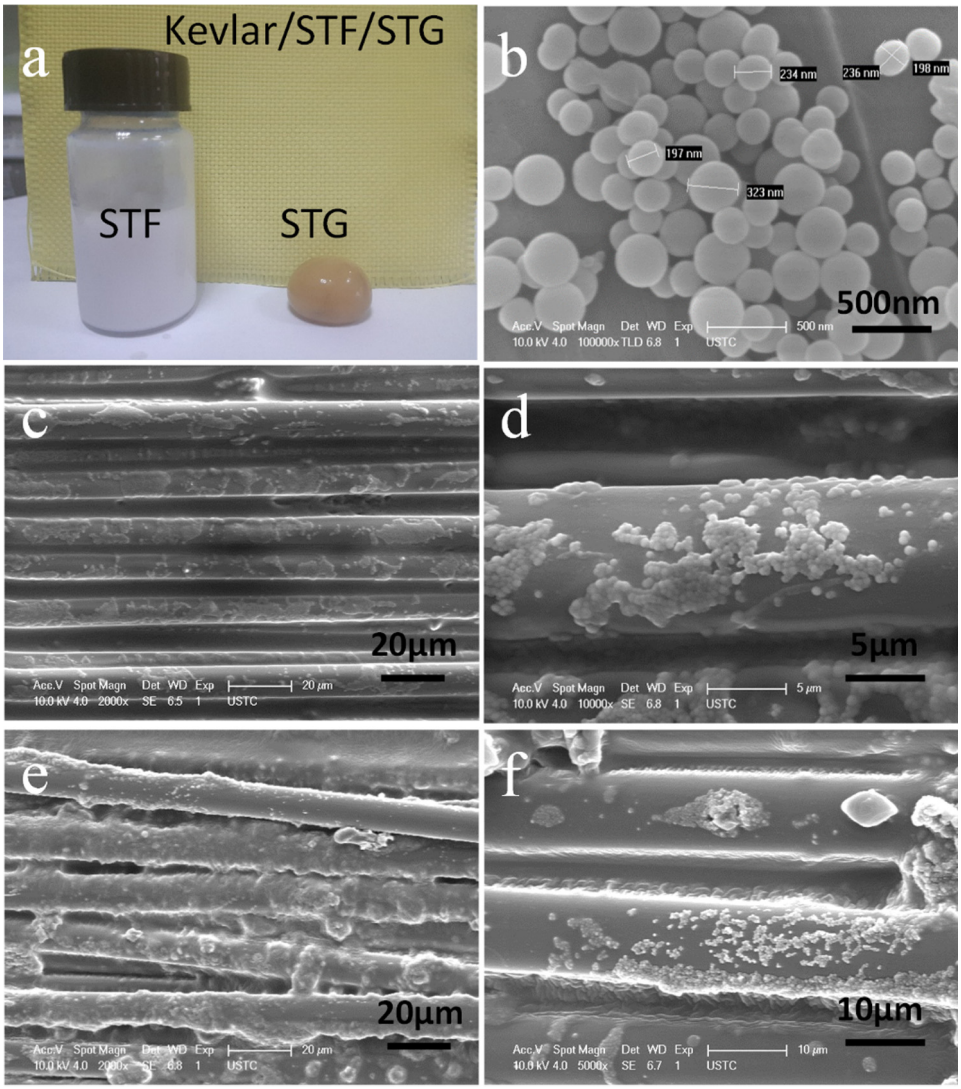

Fig. 1. Macroscopic images of STF, STG, and Kevlar/STF/STG composite (a); SEM image of silica particles in STF (b), Kevlar/STF composite (c and d), and Kevlar/STF/STG composite (e and f). (For interpretation of the references to colour in this figure legend, the reader is referred to the web version of this article.)

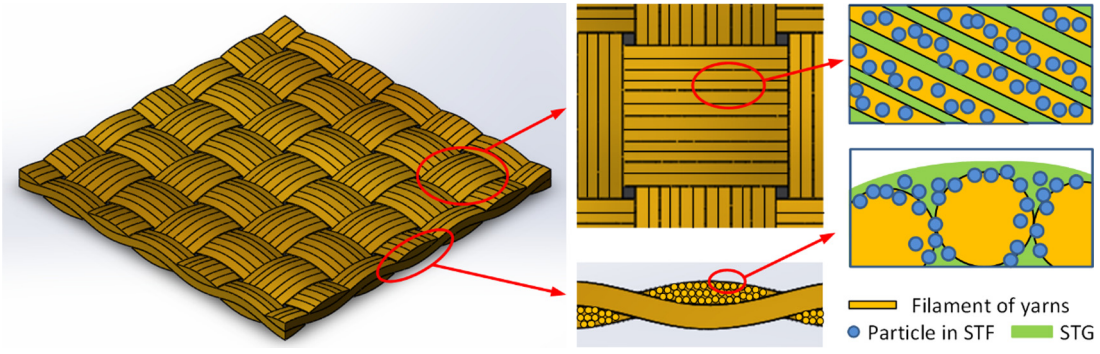

Fig. 2. The cross section of the yarns of Kevlar/STF/STG and the partial magnification. One yarn of the fabric is made up of a number of filaments, and the STF and STG are distributed between the filaments. (For interpretation of the references to colour in this figure legend, the reader is referred to the web version of this article.)

(defined as Sample 1–6). It should be noted that the weight of STF in Sample 4 was slightly higher than that of Sample 3 due to the small amount of STF was shedding during STG coating. The tests were performed on MTS Criterion™ Model 43. Fig. 4a showed the schematic diagram. The bottom of the rectangular fabric was clamped. One of the longitudinal yarns was fixed on the movable grip. The upper grip pulled the yarn out of the fabric at a constant speed of 10, 50, 100, 200 mm/min and the force *vs.* displacement curves were recorded.

2.5. SHPB test

The compressive properties of fabric composites under impact were tested by SHPB at the bar speed of 7.5 m/s. The specimens

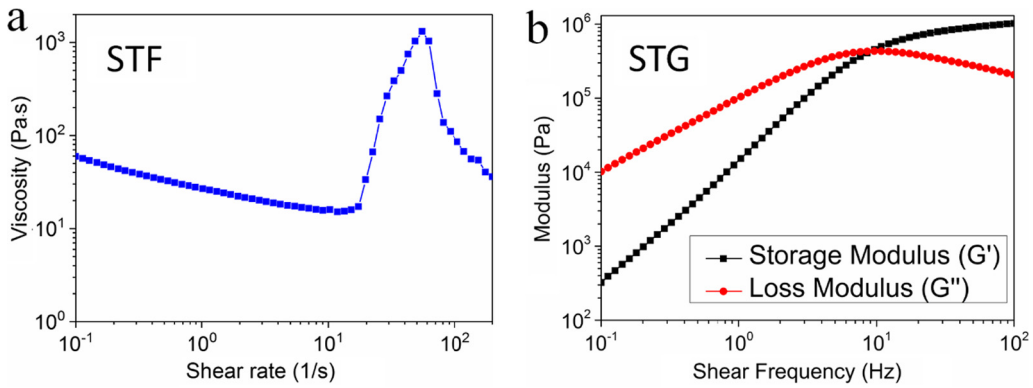

Fig. 3. The viscosity *vs.* shear rate curve of STF (the colloidal silica nanoparticles in PEG200, 60 vol%) under steady shear (a); storage modulus and loss modulus of STG under dynamic oscillatory shear (γ = 1%) (b). (For interpretation of the references to colour in this figure legend, the reader is referred to the web version of this article.)

Table 1
The composition and mass ratio of different composite fabrics that participated in the pull-out test, defined as Sample 1–6.

	Kevlar	STF	STG	PEG200	Abbreviation
Sample 1	1	–	–	–	Neat Kevlar
Sample 2	1	–	–	0.37	Kevlar/PEG200(0.37)
Sample 3	1	0.43	–	–	Kevlar/STF(0.43)
Sample 4	1	0.46	0.40	–	Kevlar/STF(0.46)/STG(0.40)
Sample 5	1	0.89	–	–	Kevlar/STF(0.89)
Sample 6	1	0.93	0.38	–	Kevlar/STF(0.93)/STG(0.38)

were composed of five layers and the surface density of Kevlar/STF (0.36), Kevlar/STG(0.36), Kevlar/STF(0.27)/STG(0.09) was about 36% larger than the neat Kevlar. As shown in Fig. 4b, the incident bar was struck to produce an elastic wave. When the incident wave (ε_i) reached the specimen-bar interface, part of it was reflected to form a reflected wave (ε_r), and the other part passed through the specimen as a transmitted wave (ε_t). ε_i, ε_r, ε_t were measured by strain gauges that attached to the bars. In this experiment, the cross-sectional area of the bar and the specimen was the same. According to one-dimensional stress wave theory,

$$\sigma(t) = E_b \varepsilon_t(t) \tag{1}$$

$$\varepsilon(t) = -\frac{2C_b}{l_s}\int_0^t \varepsilon_r(T)dT \tag{2}$$

where E_b was the elastic modulus of the bar, C_b was the elastic wave speed in the bar, l_s was the thickness of the specimen and t was the pulse length. By eliminating the time term of Eqs. (1) and (2), the stress-strain curves were obtained.

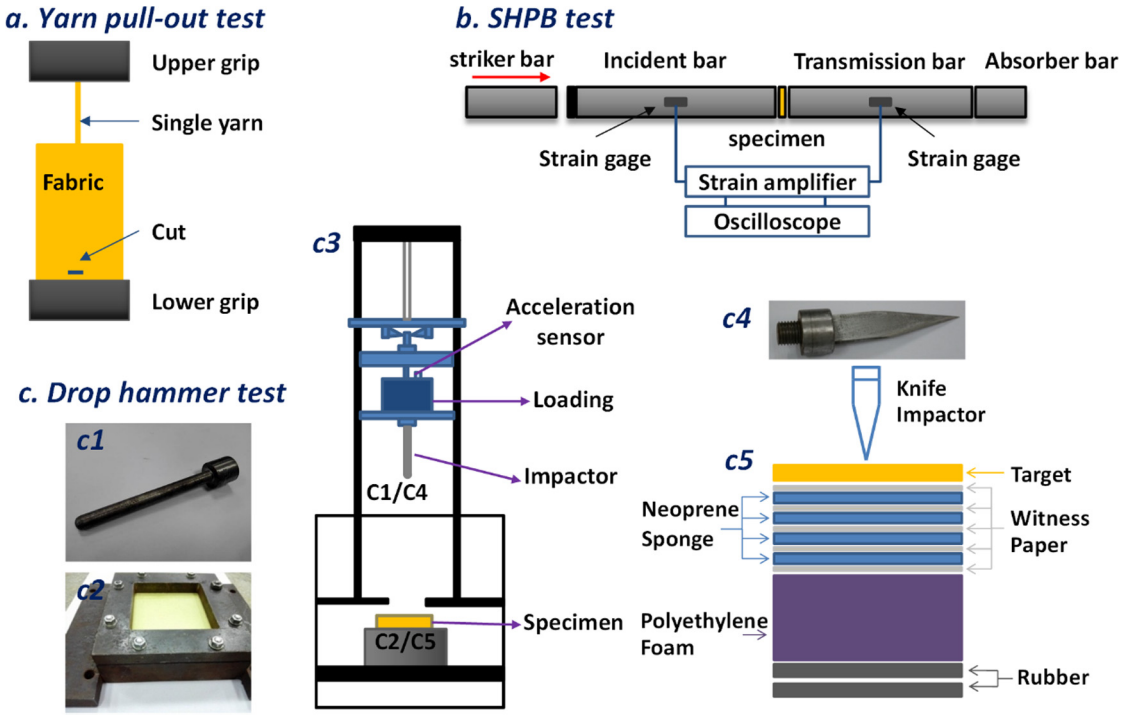

Fig. 4. Schematic illustration of experimental equipment. (a) Yarn pull-out test, (b) a modified SHPB system, (c) impact test on the drop hammer, a steel rounded tip rod (c1) matched to the fabric holder (c2), and a knife (c4) matched to the backing material (c5). (For interpretation of the references to colour in this figure legend, the reader is referred to the web version of this article.)

2.6. Drop hammer test

The failure mode of the fabric composites impacted by a rod penetration was studied on a drop hammer. A steel rounded tip rod with a diameter of 10 mm and a length of 105 mm was used as the impactor (Fig. 4c1). The single layer specimen of 12.5 × 12.5 mm^2 was securely clamped between two steel plates by eight screws, and only 9.0 × 9.0 mm^2 central area of the fabric subjected to the impact (Fig. 4c2). The neat Kevlar, Kevlar/STF(0.09), Kevlar/STF(0.09)/STG(0.09) and Kevlar/STF(0.09)/STG(0.21) (hlm) were tested. In Fig. 4c3, a total of 4 kg loading dropped freely from the height of 750 mm, which equaled to the impact speed of 3.83 m/s. The acceleration sensor was set on the impact head, and the oscilloscope recorded the change of the acceleration during the puncture process.

The knife cutting test was also carried out on the drop hammer (Fig. 4c3). According to the NIJ Standard 0115.0 [29] for stab resistance of body armor, the impactor that "knife blade S1" was used (Fig. 4c4). The knife loading 2.2 kg dropped from the height varying from 0.10 m to 0.50 m. Several layers of fabric were placed on the backing material, of which five layers of witness papers and four neoprene sponge were stacked layer-by-layer (Fig. 4c5). The number of witness paper layers punctured by the knife quantified the depth at which the backing material was penetrated to measure the impact resistance of the fabric.

3. Results and discussion

3.1. Yarn pull-out test

When the yarn in the fabric was pulled out, it would be hindered by the friction of the surrounding yarns. The surface of the neat Kevlar yarns was relatively smooth, thus the friction was low and the pull-out force was hardly dependent on the pull speed (Fig. 5a). When the fabric was doped with STF or STG, the friction was increased and the pull-out force was changed. Fig. 5b showed the speed *vs.* force curve of the Kevlar/STF (Sample 5 in Table 1). At low pull-out speed of 10 and 50 mm/min, the force was kept at a low level without showing any enhancement and this phenomenon was similar to neat Kevlar (Fig. 5a). However, when the pull-out speed was 100 mm/min, the peak of pull-out force increased to 6.17 N, which was several times larger than that of the low-speed state. The Sample 3 also displayed this sudden enhancement. It could be seen that the STF was mainly effectively worked in the dynamic process when the speed reached to a critical value. In comparison to Sample 3, the maximum force of Sample 5 was twice larger at the same speed of 100 mm/min (Fig. 5d). This result demonstrated that the fabric with higher content of STF exhibited larger friction, so macroscopic pull-out force increased with the microscopic particle-induced resistance. The PEG200 was used as the dispersion medium of STF, however, the pull-out force of Sample 2 (Kevlar/PEG200) showed a similar performance to neat fabric, and even the force decreased at low speed. Therefore, the shear thickening effect and the SiO_2 particle friction must be responded for the force increment in Kevlar/STF.

Sample 4 and Sample 6 were the Kevlar/STF/STG composites with different STF component. At the low speed of 10 mm/min, the peak force of Sample 4 reached as high as 11.6 N (Fig. 5c). When the speed increased, the peak force increased, which must be originated from the shear thickening effect. The STF content in Sample 6 (0.93) was higher than Sample 4 (0.46), thus Sample 6 possessed a larger maximum pull-out force (23.5 N) than Sample 4 (15.3 N) at the speed of 100 mm/min (Fig. 5d). Here, the weight of STF and STF/STG were the same in Sample 4 and 5. Obviously,

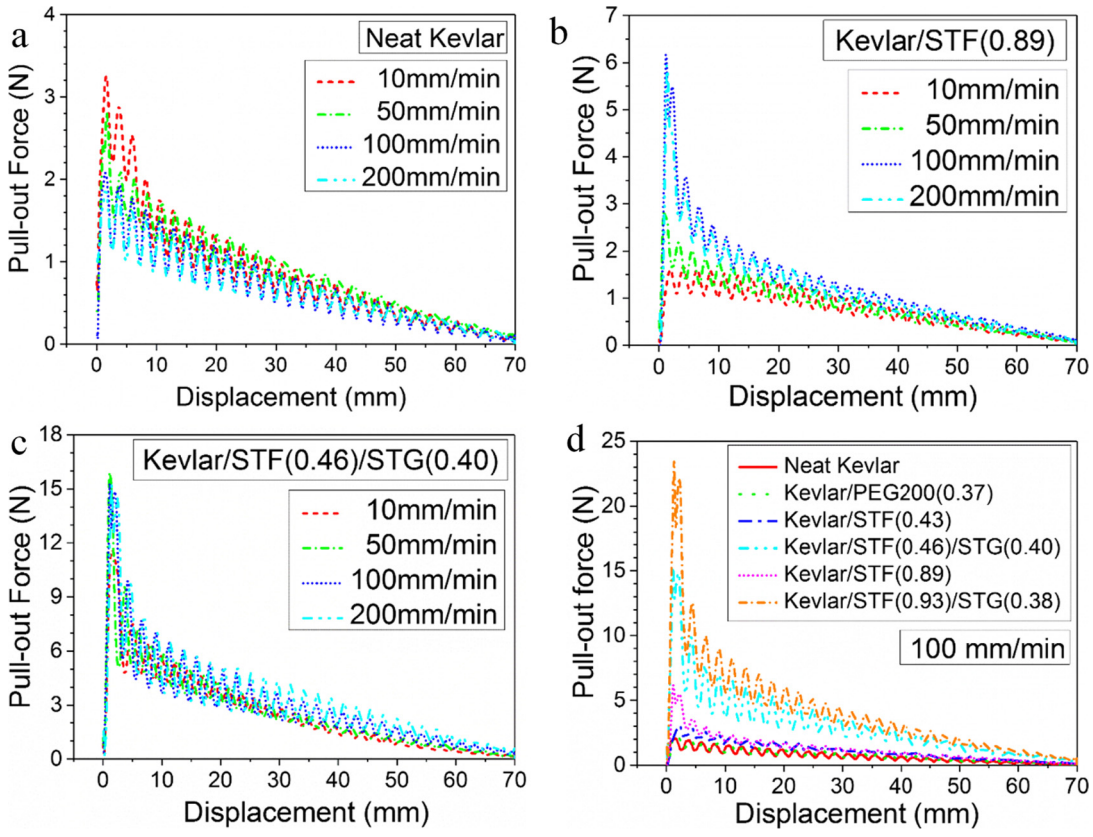

Fig. 5. Pull the yarn at a constant speed of 10, 50, 100, 200 mm/min, the yarn pull-out force *vs.* displacement curves of neat Kevlar (a), Kevlar/STF(0.89) (b), Kevlar/STF(0.46)/STG(0.40) (c), and curves of different fabric composite at the speed of 100 mm/min (d). (For interpretation of the references to colour in this figure legend, the reader is referred to the web version of this article.)

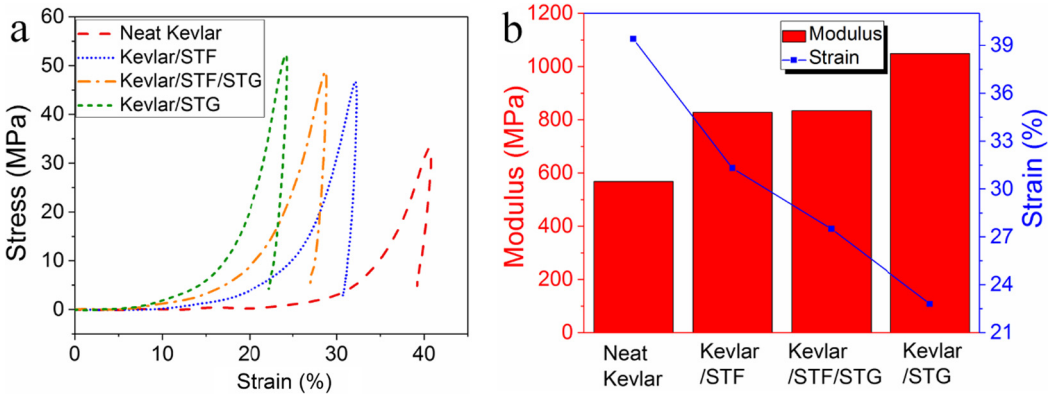

Fig. 6. The SHPB test of neat Kevlar and Kevlar impregnated with STF and STG at the impact speed of 7.5 m/s. The stress-strain curves (a), the maximum elastic modulus and the corresponding strain (b) of neat Kevlar, Kevlar/STF(0.36), Kevlar/STF(0.27)/STG(0.09) and Kevlar/STG(0.36). (For interpretation of the references to colour in this figure legend, the reader is referred to the web version of this article.)

Sample 4 had a larger pull-out resistance (15.3 N) than Sample 5 (6.2 N). It was found that the STG could greatly restrict the yarn movement, thus it showed a significant increasing effect on the peak of pull-out force. As shown in the SEM image (Fig. 1c and d), the STF and STG surrounded the yarns. When the yarns were pulled from the fabrics, the shear thickening of STF and shear stiffening of STG were occurred and led to a hindering effect. In additionally, the STF and STG additives increased the roughness of the yarn surface, thus the friction between the yarns and fabrics increased. Based on the above analysis, it can be concluded that both the STG and STF worked together to limit the sliding of the yarns.

3.2. SHPB test

The modified SHPB system was used to investigate the compressibility of the as-prepared composite fabrics and the stress-strain curves were calculated by Eqs. (1) and (2). During the measurement, the multi-layer fabric was compacted at the beginning. At this stage, the stress increased slowly with increasing of the strain. When the gap between the fabric layers was squeezed out, the stress began to rapidly rise. The rapid rise was nearly linear and the slope represented the elastic modulus of the composite fiber. Fig. 6b showed the maximum value of the elastic modulus and the corresponding strain of Kevlar/STF and Kevlar/STF/STG. The difference in the modulus was not significant, but the trend of the corresponding strain was obvious.

In Fig. 6a, keeping the bar speed of 7.5 m/s, the maximum stress corresponding to Kevlar/STG(0.36), Kevlar/STF(0.27)/STG(0.09), Kevlar/STF(0.36), and neat Kevlar was 52.0, 48.8, 46.7 and 33.1 MPa, respectively, while the corresponding strain was 0.24, 0.29, 0.32 and 0.41. Clearly, the STG exhibited a higher enhancement than the others when exposed to the same strain. The compressibility of the multi-layer Kevlar/STG(0.36) was smaller and the modulus was larger, which provided guidance for subsequent impact test. It should be noted that stress still could be increased if subjected to a larger impact speed. In this work, our instrument could not give a large enough impact velocity for rupturing the Kevlar fiber. Therefore, the maximum yield stress of the material was not measured due to the limitation of experiment.

3.3. Drop hammer test

The anti-impact performance of the composite fabrics was also tested by a drop hammer. The acceleration-time relationship was recorded during the penetration process, and the force-displacement curves could be obtained by mathematical integration (Fig. 7a). In comparison to neat Kevlar (919 N), the maximum force of the Kevlar/STF(0.09) increased dramatically to 2226 N. Moreover, the deformable displacement changed from 15.8 mm to 19.3 mm, while the weight of the Kevlar/STF was only 9.2% larger than the neat Kevlar. The morphology of the damaged fabric after impact was recorded. It was obvious that the yarns of neat Kevlar were separated by the penetration, and the two vertical main yarns were pulled out (Fig. 7e). As discussed in the above yarn pull-out test, neat Kevlar yarns could be pulled out with small force, thus the resistance between the yarns was poor. Near the impact point, the yarns were partially pulled out and surrounded the penetrator to form a "window". In contrast, the yarns fracture with an appropriate amount of filaments pulled out was the main damage of the Kevlar/STF (Fig. 7f). In consideration of the failure mode and the increased impact force, it can be understood that STF increased the sliding resistance and limited the relative movement of filaments and yarns, so more fabric yarns and filaments were loaded under impact. As described by Majumdar, the entire fabric but not just the primary yarn was participated in load bearing [30]. When the weight of the STF in Kevlar was large enough to cause the frictional resistance to be sufficiently large, the yarns would rupture before sliding. In this case, the failure form of the fabric would be the breakage, and then the higher STF increment would not be able to play a better role in that time.

Besides enhancing the impact resistance force of Kevlar/STF/STG, the STG also significantly increased the deformation time and displacement (Fig. 7a). As shown in Fig. 7g, the failure mode of Kevlar/STF/STG was still the rupture of the yarns. Fig. 7b showed the force *vs.* time curves of Kevlar/STF(0.09) and Kevlar/STF(0.09)/STG(0.09) during the rod penetration. The curve could be divided into three zones, the de-crimping and elastic elongation of the yarns (zone I), the oscillation and rise of the curve caused by the addition of additives to the yarns (zone II), and the failure zone (zone III). As shown in zone II, both the STF and STF/STG exhibited a similar effect on the maximum force. However, the STG prolonged the break time and it was found the unloading start time changed from 4.4 ms (Kevlar/STF) to 4.8 ms (Kevlar/STF/STG).

The energy dissipation was also calculated by integrating the force-displacement curves. In Fig. 7d, the energy dissipation ranged from 7.71 J of neat Kevlar, to 15.96 J of Kevlar/STF(0.09) and 19.44 J of Kevlar/STF(0.09)/STG(0.09). This result indicated that the STF and STG significantly increased the energy dissipation of Kevlar. Compared to Kevlar/STF, the force of Kevlar/STF/STG oscillated heavier and it consumed more energy in zone III (Fig. 7a and b). It was reported that the higher coefficient of friction

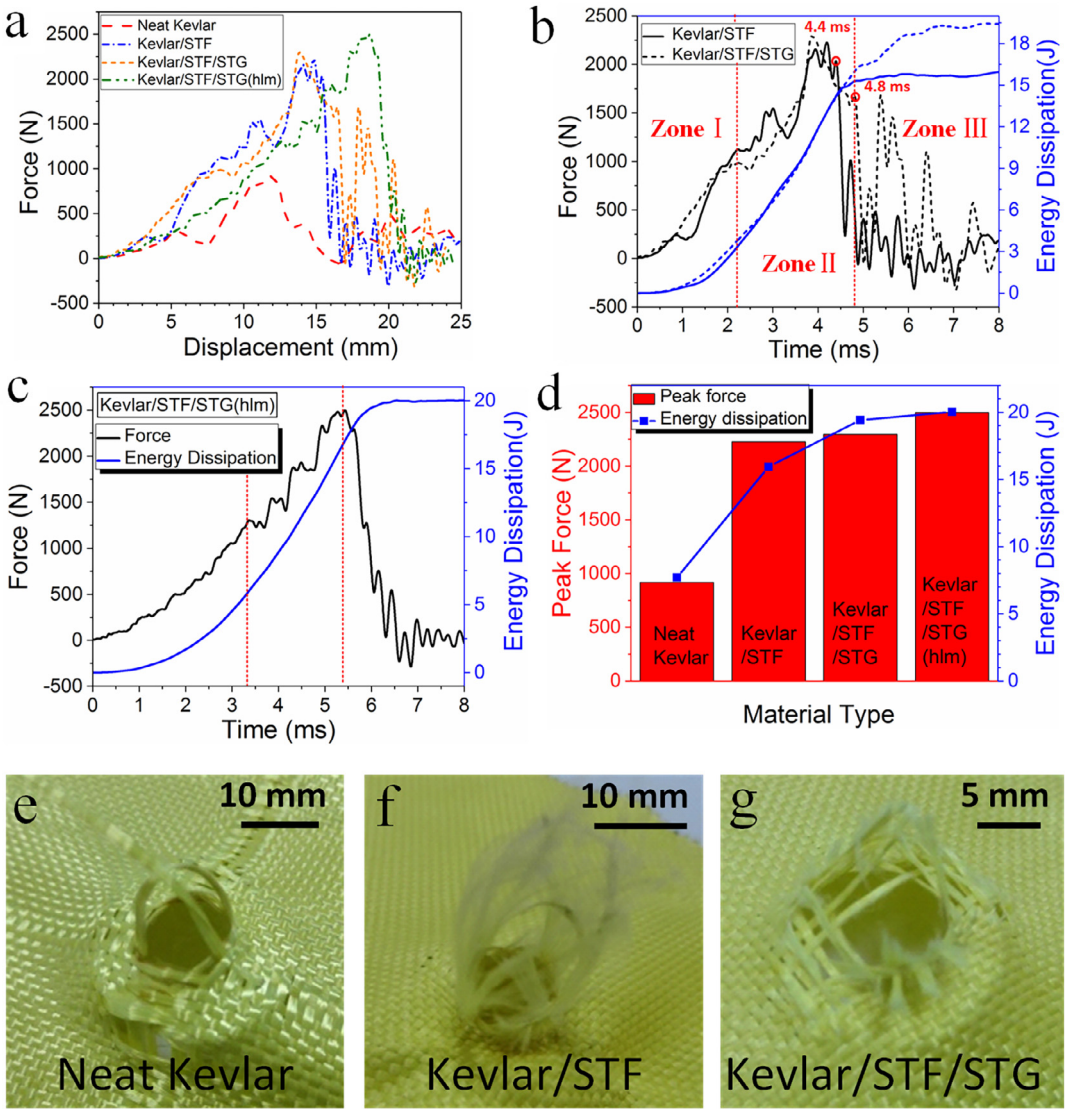

Fig. 7. Force-displacement relationships under the impact of a rounded tip rod at an initial velocity of 3.83 m/s with a loading of 4 kg (a). The force *vs.* time curves of Kevlar/STF(0.09), Kevlar/STF(0.09)/STG(0.09) (b), and Kevlar/STF(0.09)/STG(0.21) (hlm) (c). The energy dissipation during the impact process and the peak force (d). The morphology of the damaged fabric that neat Kevlar (e), Kevlar/STF (f), and Kevlar/STF/STG (g). (For interpretation of the references to colour in this figure legend, the reader is referred to the web version of this article.)

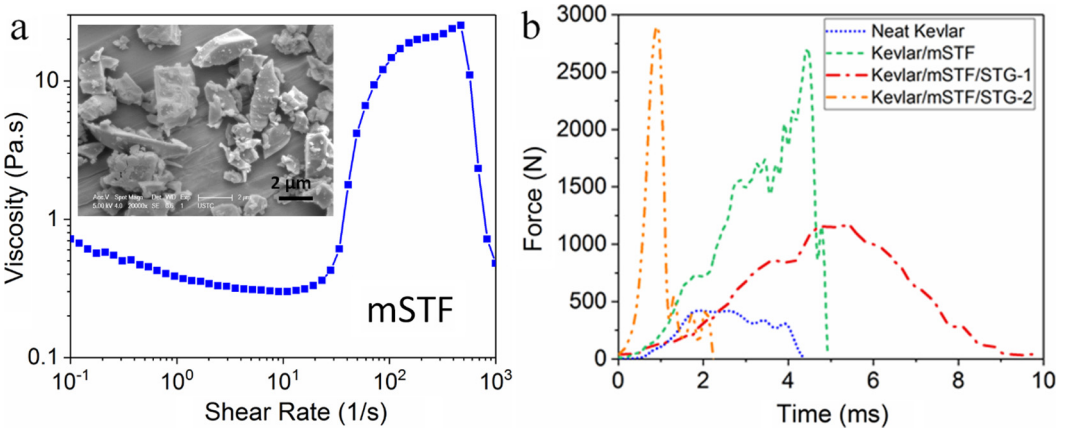

Fig. 8. The viscosity *vs.* shear rate curve of mSTF (the micron-sized silica particles in EG, 56 vol%) under steady shear. Inset: SEM image of the silica particles in mSTF having an average diameter of 2.6 μm (a). Force *vs.* time curves under the impact of a rounded tip rod at an initial velocity of 3.83 m/s with a loading of 4 kg (b). (For interpretation of the references to colour in this figure legend, the reader is referred to the web version of this article.)

would cause more yarns and filaments to participate in load-bearing [31]. As we know, the STG significantly increased the friction between the yarns. Thus, the impact was dispersed and the energy was consumed in both of the Kevlar/STF and Kevlar/STF/STG.

In this work, different kinds of STFs were also applied to investigate the generality of anti-impact performance. The mSTF prepared by dispersing micron-sized silica particles in EG was used. Fig. 8 showed the rheology property of mSTF and drop hammer test of the final Kevlar/mSTF. Keeping other parameters as constants, the neat Kevlar and Kevlar/mSTF(0.12) were tested, and they were penetrated and destroyed during the process. However, the Kevlar/mSTF(0.12)/STG(0.12) after the first impact was not completely penetrated and a second impact was followed. The two acceleration signals were marked as Kevlar/mSTF/STG-1 and Kevlar/mSTF/STG-2. Fig. 8b demonstrated that the first impact caused a large displacement and a low peak force. Under the second impact, the force increased rapidly and reached a large peak, and then the fabric was destroyed. The above result further validated that STG-strengthened fabric had a stronger impact resistance.

3.4. The influence of different configurations of Kevlar/STF/STG

In this work, STG was also doped into Kevlar/STF by hand layup method (hlm), and the final sample was labeled as Kevlar/STF/STG (hlm). In comparison to the Kevlar/STF(0.09)/STG(0.09), the force *vs.* displacement curve of Kevlar/STF(0.09)/STG(0.21) (hlm) was relatively gentle (Fig. 7a and c), while the maximum force was larger and the deformation displacement was greater. This result was because the STG was stiffened as the force increased (Fig. 2b), then storage modulus was significant increased. In the hlm method, the STG showed an obvious strengthening effect. When subjected to impact, STG first met the external force, dissipated part of energy to slow down the impactor and thus the subsequent impact on the fabric was weakened. In this case, the anti-impact area increased and duration was prolonged, therefore, more energy was dissipated (20.03 J in Fig. 7d).

In addition, the knife stab resistance performance of the Kevlar/mSTF/STG(hlm) was studied. Several layers of neat Kevlar, Kevlar/mSTF/STG and Kevlar/mSTF/STG(hlm) were placed on the backing material (Fig. 4c5). Table 2 showed the number of layers and stacking arrangement, and the samples marked as target A–D was schematic illustrated in Fig. 9a. Record the layers' number of witness paper be cut in the backing material by the knife. The surface density of the monolayer Kevlar/mSTF was 10% higher than that of neat Kevlar. Thus, the target A with 10-layer different composite fabric was slightly lower than the target D with 11 layers. In Fig. 9b, when the drop height of the knife was 200 mm, the witness papers of target D were completely destroyed (5 layers), while the papers of target A reached the same degree of damage at the height of 400 mm. It could be seen that the mSTF reduced the puncture layers' number of the backing material under the same impact energy, thus significantly improved the knife stab resistance performance of neat Kevlar.

The influence of STG on the knife stab resistance performance was then studied. Compared with target A, target B has 2 additional STG layers in the outer part of the sandwich structure. When the knife fell from 400 mm, target A was penetrated with 5 paper layers. However, only 4 layers were penetrated for the target B when the height was 500 mm. Obviously, the penetrating papers layers for target B was less than that of target A at the same drop height, which demonstrated that the STG played a significant role in the strengthening process. However, the protective effect of target C containing 4 STG layers was the same as target B with 2 STG layers, thus more STG could not lead to a better result and the optimum value still needed further exploration.

Based on the above analysis, it was found that the "hand layup method" could improve the resist ability against knife cutting. However, the weight gain was higher than that of "dip and dry

Table 2
The number of layers and stacking arrangement of neat Kevlar, Kevlar/mSTF and STG. The samples were marked as target A-D. In the description of the placement of fabric, "F'", "K" and "G" represented the monolayer Kevlar/mSTF, neat Kevlar and STG, respectively.

Target	Kevlar/mSTF (F′)	Neat Kevlar (K)	STG (G)	Description
A	6 layers	4 layers	–	2K/6F′/2K
B	6 layers	4 layers	2 layers	2K/1G/6F′/1G/2K
C	6 layers	4 layers	4 layers	2K/1G/3F′/2G/3F′/1G/2K
D	0 layers	11 layers	–	11K

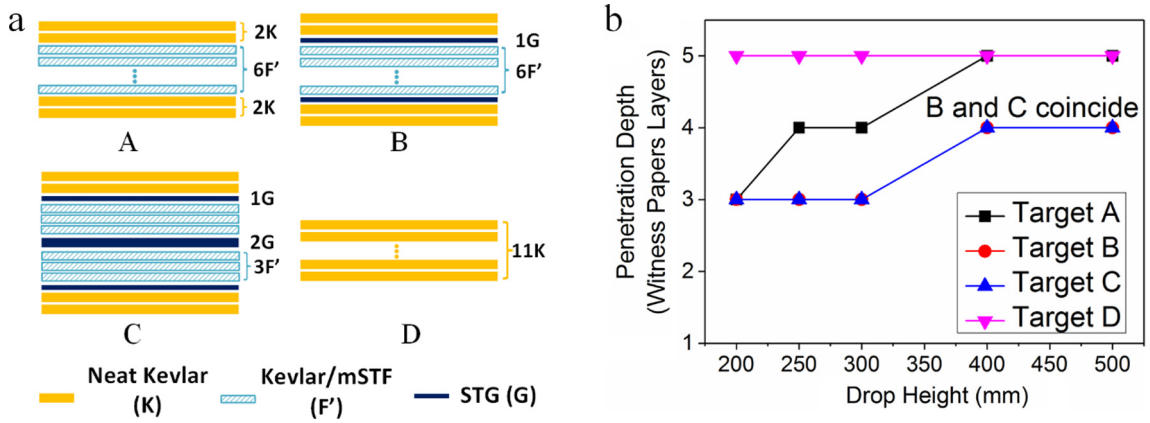

Fig. 9. Schematic of the targets A–D with different stacking arrangement (a). The knife stab resistance performance of targets A–D (b). (For interpretation of the references to colour in this figure legend, the reader is referred to the web version of this article.)

method" although it is more simple and quicker. To this end, both methods had their own advantages and disadvantages, they could bring excellent enhancement to the fabric in the corresponding area.

4. Conclusions

In this work, Kevlar/STF/STG composites were developed for high protection performance. Besides improving the stability, STG assisted STF together to improve the impact resistance performance of the fabric. The STG effectively incorporated into the gap of the filaments, and increased the friction when the yarn sliding. The SHPB test indicated that the STG reduced the compressibility of multi-layer fabric composite and increased the modulus of the yarns. The impact test carried out on the drop hammer demonstrated that the STG enhanced the impact resistance force, increased the deformation displacement, and improved the energy dissipation. The reason for the better protective effect in Kevlar/STF/STG was that STG assisted STF to limit the sliding of the yarns, increased the strength of the yarns, and mobilized more yarns around to share the impact force. Besides, different preparation method for Kevlar/STF/STG was compared and experiments confirmed that the STG could enhance the protective effect and the "hand layup method" led to a better knife stab resistance performance. In general, the light-weight shear-thickening materials enhanced Kevlar fabric exhibit strong impact resistance and they are expected to have broad potential in the soft body armor.

Acknowledgements

This work was supported by the National Natural Science Foundation of China [Grant No. 11372301, 11772320], the Strategic Priority Research Program of the Chinese Academy of Sciences [Grant No. XDB22040502], and the Fundamental Research Funds for the Central Universities [WK2480000002]. This work was also supported by the Collaborative Innovation Center of Suzhou Nano Science and Technology.

References

[1] Srivastava A, Majumdar A, Butola BS. Improving the impact resistance of textile structures by using shear thickening fluids: a review. Crit Rev Solid State Mater Sci 2012;37(2):115–29.
[2] Lee YS, Wetzel ED, Wagner NJ. The ballistic impact characteristics of Kevlar® woven fabrics impregnated with a colloidal shear thickening fluid. J Mater Sci 2003;38(13):2825–33.
[3] Brown E, Jaeger HM. Shear thickening in concentrated suspensions: phenomenology, mechanisms and relations to jamming. Rep Prog Phys 2014;77(4):046602.
[4] Barnes HA. Shear-thickening ("dilatancy") in suspensions of nonaggregating solid particles dispersed in Newtonian liquids. J Rheol 1989;33(2):329–66.
[5] Zhang XZ, Li WH, Gong XL. The rheology of shear thickening fluid (STF) and the dynamic performance of an STF-filled damper. Smart Mater Struct 2008;17(3):035027.
[6] Tan ZH, Zuo L, Li WH, Liu LS, Zhai PC. Dynamic response of symmetrical and asymmetrical sandwich plates with shear thickening fluid core subjected to penetration loading. Mater Des 2016;94:105–10.
[7] Hassan TA, Rangari VK, Jeelani S. Synthesis, processing and characterization of shear thickening fluid (STF) impregnated fabric composites. Mater Sci Eng, A 2010;527:2892–9.
[8] Decker MJ, Halbach CJ, Nam CH, Wagner NJ, Wetzel ED. Stab resistance of shear thickening fluid (STF)-treated fabrics. Compos Sci Technol 2007;67:565–78.
[9] Gong X, Xu Y, Zhu W, Xuan S, Jiang W, Jiang W. Study of the knife stab and puncture-resistant performance for shear thickening fluid enhanced fabric. J Compos Mater 2014;48(6):641–57.
[10] Lu Z, Jing X, Sun B, Gu B. Compressive behaviors of warp-knitted spacer fabrics impregnated with shear thickening fluid. Compos Sci Technol 2013;88:184–9.
[11] Lu Z, Wu L, Gu B, Sun B. Numerical simulation of the impact behaviors of shear thickening fluid impregnated warp-knitted spacer fabric. Composites Part B 2015;69:191–200.
[12] Haro EE, Szpunar JA, Odeshi AG. Ballistic impact response of laminated hybrid materials made of 5086–H32 aluminum alloy, epoxy and Kevlar® fabrics impregnated with shear thickening fluid. Composites Part A 2016;87:54–65.
[13] Park Y, Kim YH, Baluch AH, Kim CG. Numerical simulation and empirical comparison of the high velocity impact of STF impregnated Kevlar fabric using friction effects. Compos Struct 2015;125:520–9.
[14] Haris A, Lee HP, Tay TE, Tan VBC. Shear thickening fluid impregnated ballistic fabric composites for shock wave mitigation. Int J Impact Eng 2015;80:143–51.
[15] Feng X, Li S, Wang Y, Wang Y, Liu J. Effects of different silica particles on quasi-static stab resistant properties of fabrics impregnated with shear thickening fluids. Mater Des 2014;64:456–61.
[16] Kalman DP, Merrill RL, Wagner NJ, Wetzel ED. Effect of particle hardness on the penetration behavior of fabrics intercalated with dry particles and concentrated particle-fluid suspensions. ACS Appl Mater Int 2009;1(11):2602–12.
[17] Li W, Xiong D, Zhao X, Sun L, Liu J. Dynamic stab resistance of ultra-high molecular weight polyethylene fabric impregnated with shear thickening fluid. Mater Des 2016;102:162–7.
[18] Gürgen S, Kuşhan MC. The stab resistance of fabrics impregnated with shear thickening fluids including various particle size of additives. Composites Part A 2017;94:50–60.
[19] Hasanzadeh M, Mottaghitalab V, Babaei H, Rezaei M. The influence of carbon nanotubes on quasi-static puncture resistance and yarn pull-out behavior of shear-thickening fluids (STFs) impregnated woven fabrics. Composites Part A 2016;88:263–71.
[20] Laha A, Majumdar A. Interactive effects of p-aramid fabric structure and shear thickening fluid on impact resistance performance of soft armor materials. Mater Des 2016;89:286–93.
[21] Park JL, Yoon BI, Paik JG, Kang TJ. Ballistic performance of p-aramid fabrics impregnated with shear thickening fluid; Part II - effect of fabric count and shot location. Text Res J 2012;82(6):542–57.
[22] Wang Y, Wang S, Xu C, Xuan S, Jiang W, Gong X. Dynamic behavior of magnetically responsive shear-stiffening gel under high strain rate. Compos Sci Technol 2016;127:169–76.
[23] Tian TF, Li WH, Ding J, Alici G, Du H. Study of shear-stiffened elastomers. Smart Mater Struct 2012;21(12):125009.
[24] Golinelli N, Spaggiari A, Dragoni E. Mechanical behaviour of magnetic Silly Putty: viscoelastic and magnetorheological properties. J Intell Mater Syst Struct; 2015: 1045389X15591655.
[25] Jiang W, Gong X, Wang S, Chen Q, Zhou H, Jiang W, et al. Strain rate-induced phase transitions in an impact-hardening polymer composite. Appl Phys Lett 2014;104(12):121915.
[26] Kulikov O, Hornung K. Novel processing aid based on modified Silly Putty. J Vinyl Addit Technol 2006;12(3):131–42.
[27] Wang S, Jiang W, Jiang W, Ye F, Mao Y, Xuan S, et al. Multifunctional polymer composite with excellent shear stiffening performance and magnetorheological effect. J Mater Chem C 2014;2(34):7133–40.
[28] Wang S, Xuan S, Liu M, Bai L, Zhang S, Sang M, et al. Smart wearable Kevlar-based safeguarding electronic textile with excellent sensing performance. Soft Matter 2017;13:2483–91.
[29] Standard NIJ. 0115.00. Stab resistance of personal body armor. Washington: National Institute of Justice; 2000.
[30] Majumdar A, Butola BS, Srivastava A. An analysis of deformation and energy absorption modes of shear thickening fluid treated Kevlar fabrics as soft body armour materials. Mater Des 2013;51:148–53.
[31] Briscoe BJ, Motamedi F. The ballistic impact characteristics of aramid fabrics: the influence of interface friction. Wear 1992;158(1–2):229–47.